The Journal of Physiology

BK channels mediate a novel ionic mechanism that regulates glucose-dependent electrical activity and insulin secretion in mouse pancreatic β-cells

Khaled M. Houamed[1,2], Ian R. Sweet[3] and Leslie S. Satin[1,2]

[1]*Department of Pharmacology and* [2]*Brehm Diabetes Center, University of Michigan Medical School, Ann Arbor, MI, USA*
[3]*Diabetes and Obesity Center, University of Washington, Seattle, WA, USA*

BK channels are large unitary conductance K^+ channels cooperatively activated by intracellular calcium and membrane depolarisation. We show that BK channels regulate electrical activity in β-cells of mouse pancreatic islets exposed to elevated glucose. In 11.1 mM glucose, the non-peptidyl BK channel blocker paxilline increased the height of β-cell action potentials (APs) by 21 mV without affecting burst- or silent-period durations. In isolated β-cells, paxilline increased AP height by 16 mV without affecting resting membrane potential. In voltage clamp, paxilline blocked a transient component of outward current activated by a short depolarisation, which accounted for at least 90% of the initial outward K^+ current. This BK current (I_{BK}) was blocked by the Ca^{2+} channel blockers Cd^{2+} (200 μM) or nimodipine (1 μM), and potentiated by FPL-64176 (1 μM). I_{BK} was also 56% blocked by the BK channel blocker iberiotoxin (100 nM). I_{BK} activated more than 10-fold faster than the delayed rectifier I_{Kv} over the physiological voltage range, and partially inactivated. An AP-like command revealed that I_{BK} activated and deactivated faster than I_{Kv} and accounted for 86% of peak I_K, explaining why I_{BK} block increased AP height. A higher amplitude AP-like command, patterned on an AP recorded in 11.1 mM glucose plus paxilline, activated 4-fold more I_{Kv} and significantly increased Ca^{2+} entry. Paxilline increased insulin secretion in islets exposed to 11.1 mM glucose by 67%, but did not affect basal secretion in 2.8 mM glucose. These data suggest a modified model of β-cell AP generation where I_{BK} and I_{Kv} coordinate the AP repolarisation.

Abbreviations AHP, afterhyperpolarisation; AP, action potential; BK, large-conductance Ca^{2+}-activated K^+; ChTx, charybdotoxin; G_{Kv}, voltage-activated K^+ conductance; GSIS, glucose-stimulated insulin secretion; I_{BK}, large-conductance Ca^{2+}-activated K^+ current; IbTx, iberiotoxin; I_{Cav}, voltage-activated Ca^{2+} current; I_K, total outward K^+ current; I_{Kv}, voltage-activated K^+ current; Q_{Cav}, voltage-activated Ca^{2+} charge influx; RIA, radioimmunoassay; R_s, series resistance.

Introduction

Elevated ambient glucose triggers action potentials (APs) in β-cells of murine pancreatic islets (Dean & Matthews, 1968). It is thought that voltage-dependent Ca^{2+} current (I_{Cav}) underlies the AP upstroke, and delayed rectifier K^+ current (I_{Kv}, mediated mostly by K_v2.1 channels (Roe *et al.* 1996; MacDonald & Wheeler, 2003; Herrington *et al.* 2006)) drives the downstroke (Ashcroft & Rorsman, 1989; Houamed *et al.* 2004).

BK channels are K^+ channels of large unitary conductance that are activated cooperatively by elevated $[Ca^{2+}]_i$ and membrane depolarisation (Marty, 1981; Kaczorowski

et al. 1996; Vergara *et al.* 1998). This dual sensitivity allows BK channels to subserve disparate physiological functions in many cell types (Orio *et al.* 2002). BK channels vary widely in their biophysical and pharmacological properties as a result of multiple splicing of the ion-conducting α-subunit mRNA (Adelman *et al.* 1992; Butler *et al.* 1993), differential incorporation of four modulatory β-subunits (Orio *et al.* 2002), and multiple phosphorylation patterns (Yan *et al.* 2008).

Rodent β-cells and certain insulinomas express BK channels (Cook *et al.* 1984; Findlay *et al.* 1985; Satin *et al.* 1989; Tabcharani & Misler, 1989; Bokvist *et al.* 1990; Mancilla & Rojas, 1990; Smith *et al.* 1990*b*; Kukuljan

et al. 1991; Li *et al.* 1999), but the role of these channels in β-cell physiology has been controversial. Early studies and theoretical models proposed that I_{BK} regulated glucose-dependent electrical excitability in β-cells (Atwater *et al.* 1979, 1983; Chay, 1986). However, Smith *et al.* (1990b) observed that I_{BK} constituted only a minor and variable component of the depolarisation-activated I_K, concluding that it was thus unlikely to play a major role in shaping APs. Similarly, Kukuljan *et al.* (1991) reported that the I_{BK} blocker charybdotoxin (ChTx) did not affect glucose-induced APs or islet bursting, and concluded that I_{BK} did not participate in glucose-induced electrical activity. Thus, there emerged a consensus that BK channels do not significantly participate in the glucose-mediated islet electrical activity or in glucose-stimulated insulin secretion (GSIS) in mouse. However, β-cells from a $K_v2.1$ knockout mouse lacking I_{Kv} are still capable of AP repolarisation, and moreover, express a transient outward K^+ current of unknown molecular identity (Jacobson *et al.* 2007). Similarly, toxin block of β-cell $K_v2.1$ channels slowed, but did not inhibit, AP repolarisation. Further, human β-cells have recently been shown to express a robust I_{BK} whose pharmacological modulation affects both AP shape and GSIS (Braun *et al.* 2008).

The present study examines whether I_{BK} is activated in primary mouse β-cells under physiological conditions, and investigates its possible role in the control of islet electrical activity and GSIS. Preliminary results have been described previously in abstract form (Houamed & Satin, 2009).

Methods

Isolation of islets and single β-cells

Islets were isolated from adult male Swiss Webster mice as previously described (Goforth *et al.* 2002; Zhang *et al.* 2005), using a protocol approved by the University of Michigan University Committee on the Use and Care of Animals, and following published standards (Drummond, 2009). Animals were killed by neck dislocation. The pancreas was perfused through the bile duct with cold Krebs solution containing 1 mg ml^{-1} collagenase P (Roche Diagnostics, Indianapolis, IN, USA) and 0.1% bovine serum albumin (BSA), then rapidly excised, incubated at 37°C for 15 min, triturated and washed. Krebs solution contained (in mM): 137 NaCl, 5 KCl, 1.2 MgCl$_2$, 1 CaCl$_2$, 5 NaHCO$_3$, 5 glucose, 10 Hepes; pH 7.35. Single β-cells and islets were dispersed in Spinner's salts, washed with culture medium and plated onto glass coverslips. Islets and single β-cells were maintained in RPMI 1640 medium supplemented with 10% fetal calf serum and antibiotics (Invitrogen, Carlsbad, CA, USA) in 5% CO$_2$ at 37°C. Most islets and single cells were used within 24 h and 72 h,

respectively. As we have noted previously (Zhang *et al.* 2003), these culture periods did not appear to affect the electrical properties or the glucose sensitivity of islets and individual β-cells.

Electrophysiology

Single islets or coverslips with attached β-cells were placed in a $\sim$300 μl recording chamber constantly superfused, at 2 ml min^{-1} and 33.5°C, with a saline solution containing (in mM): 140 NaCl, 10 Hepes, 1 MgCl$_2$, 2.5 CaCl$_2$, 3.6 KCl, pH 7.35. Drugs and glucose were dissolved directly into the saline solution; when drugs were diluted from DMSO stocks, the highest final concentration of the solvent was <0.1%. Iberiotoxin solutions contained 0.1% BSA to prevent the toxin from sticking to the perfusion system. Glucose (11.1 mM) was added for membrane potential recording; for voltage-clamp recordings, 5 mM glucose and 200 μM tolbutamide were present. The two glucose concentrations, which have been used in β-cell studies involving measurement of membrane potential and current, Ca_i^{2+} dynamics, and insulin secretion (Gopel *et al.* 1999b; Zhang *et al.* 2005), were used to facilitate comparison with previous studies. For I_{Cav} measurements, 30 mM TEA was added to block I_K, and NaCl reduced accordingly to maintain the osmolarity of the saline solution.

Recordings utilized the perforated patch technique, using the pore-forming compounds nystatin or amphotericin-B (Falke *et al.* 1989). Pipette resistance was 1.6–4.4 MΩ when filled with a solution composed of (in mM): 76 K$_2$SO$_4$, 5 NaCl, 10 KCl, 1 MgCl$_2$, 10 Hepes, pH 7.35. For I_{Cav} measurements, Cs$_2$SO$_4$ replaced K$_2$SO$_4$. The pore formers were dissolved in DMSO at 50 μg ml^{-1} then diluted in pipette solution to a final concentration of 250 μg ml^{-1}. Pipette tips were dipped in pipette solution, then back-filled with pipette solution containing the pore former. Recordings commenced when the series resistance (R_s) was <40 MΩ; most of the remaining R_s was compensated electronically so that the voltage error generated by the largest currents was <6 mV. All salts and drugs were from Sigma (St Louis, MO, USA), except paxilline, which was from Enzo Life Sciences (Plymouth Meeting, PA, USA), and iberiotoxin, which was from AnaSpec (Fremont, CA, USA).

Functional criteria used to identify β-cells *in situ* on the surface of an islet were presence of AP bursts in 11.1 mM glucose, membrane capacitances >5.7 pF, and the absence of an early Na$^+$ current that remains activatable at physiological membrane potentials (Gopel *et al.* 1999a). Similar criteria were used to identify dissociated β-cells; in addition, we visually selected for larger cells, which were more likely to be β-cells (Leung *et al.* 2005). Data reported in the present study are based on recordings obtained from

51 isolated β-cells whose average membrane electrical capacitance was 7.86 ± 0.32 pF. The average capacitance of β-cells *in situ* in islets was 8.34 ± 0.39 pF ($n = 18$).

An EPC9 amplifier and PULSE software (HEKA, Lambrecht/Pfalz, Germany) provided stimulation and data acquisition. This study utilized four pulse protocols (P1, AP1, AP2 and IV1). P1 consisted of 40 ms depolarising pulse from -70 mV to -10 mV. AP1 and AP2 were synthetic APs patterned on β-cell APs recorded in 11.1 mM glucose without and with 1 μM paxilline, respectively (Fig. 1*D*). Each AP command consisted of a -65 mV holding potential segment followed by 14 ramps (Fig. 5*A* and *B*). IV1 consisted of 500 ms depolarising test pulses from -70 mV holding potential; test potentials were -60 mV to $+10$ mV in 10 mV increments. Linear leak and capacitive components of membrane current were subtracted by a combination of analog and digital (p/n) techniques; data traces shown in Figs 2, 5 and 6 are averages of several consecutive recordings. Data were analysed using PULSEFIT (HEKA), Igor (Wavemetrics, Lake Oswego, OR, USA), Excel (Microsoft, Redmond, WA, USA) and Prism (Graphpad, La Jolla, CA, USA). APs were analysed using Synaptosoft (Decatur, GA, USA). Recordings were corrected for a $+10.8$ to $+12.3$ mV calculated junction potential (Neher, 1992).

Insulin secretion measurements

Insulin secretion measurements were as previously described (Jung *et al.* 2009). Islets were preincubated for 60 min in Krebs–Ringer bicarbonate solution composed of (in mM): 98.5 NaCl, 4.9 KCl, 2.6 $CaCl_2$, 1.2 $MgSO_4$, 1.2 KH_2PO_4, 25.9 $NaHCO_3$, 20 Hepes, 2.8 glucose and 0.1% BSA. Batches of 10 islets were incubated for 60 min in 200 μl of RPMI 1640 media containing either 2.8 or 11.1 mM glucose, in the presence or absence of 1 μM paxilline; supernatant insulin was determined by radio-immunoassay (RIA; Linco Research Inc., St Charles, MO, USA). Determinations were in triplicate, and the experiments were repeated on three different islet preparations.

Statistics

Error bars denote S.E.M.; Student's *t* test was used to determine statistical significance.

Results

The effect of BK channel block on glucose-dependent electrical activity in islets

Islets exposed to elevated glucose generate AP bursts separated by silent intervals (Fig. 1*A*) (Henquin &

Meissner, 1984; Gopel *et al.* 1999*b*; Zhang *et al.* 2003, 2005). Slow-, fast- and mixed-bursting patterns, ranging in frequency from ~2 to ~0.2 min^{-1}, have been observed in individual islets (Zhang *et al.* 2003). We investigated the effect of 1 μM paxilline on the membrane potential of superficial β-cells ($n = 22$; average recording per cell ~25 min) on intact islets stimulated by 11.1 mM glucose (Fig. 1*A*). Paxilline is a non-peptidyl tremourogenic BK channel inhibitor with nanomolar potency (Knaus *et al.* 1994; Sanchez & McManus, 1996). As the effects of paxilline were poorly reversible, each islet or single β-cell was exposed to the drug only once.

Analysis of burst- and silent-interval durations in pooled data revealed that the pattern of alternating bursts and silent intervals was unaffected by addition of paxilline, while AP amplitude was increased dramatically. The mean burst duration was 178.29 ± 39.80 s ($n = 18$ islets) in 11.1 mM glucose, and 162.37 ± 32.14 s ($n = 17$) after paxilline addition; these values were not significantly different ($P = 0.76$). Likewise, the mean silent
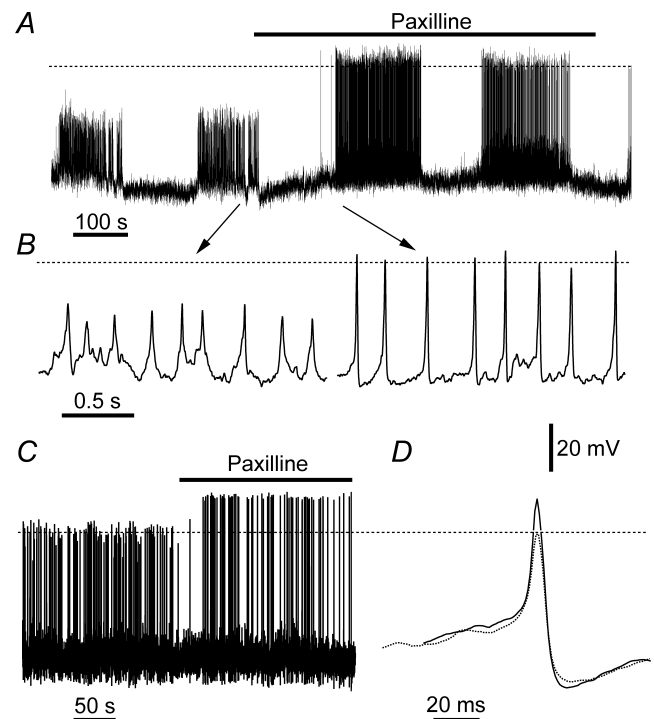

Figure 1. Effects of BK channel blocker paxilline on the electrical activity of glucose-stimulated islets and single β-cells
A, membrane potential recording in an islet exposed to 11.1 mM glucose, showing typical bursting. Paxilline (1 μM; horizontal bar) dramatically increased AP height. *B*, data from *A* on an expanded time scale. The arrows show approximate location of traces in *A*. *C*, effect of paxilline on APs of a single β-cell exposed to 1 μM paxilline in 11.1 mM glucose (denoted by the horizontal bar). *D*, two APs extracted from the trace in *C* are shown superimposed; dotted and continuous traces were recorded in the absence and presence of paxilline, respectively. Dashed lines denote 0 mV level; all panels have the same voltage calibration.
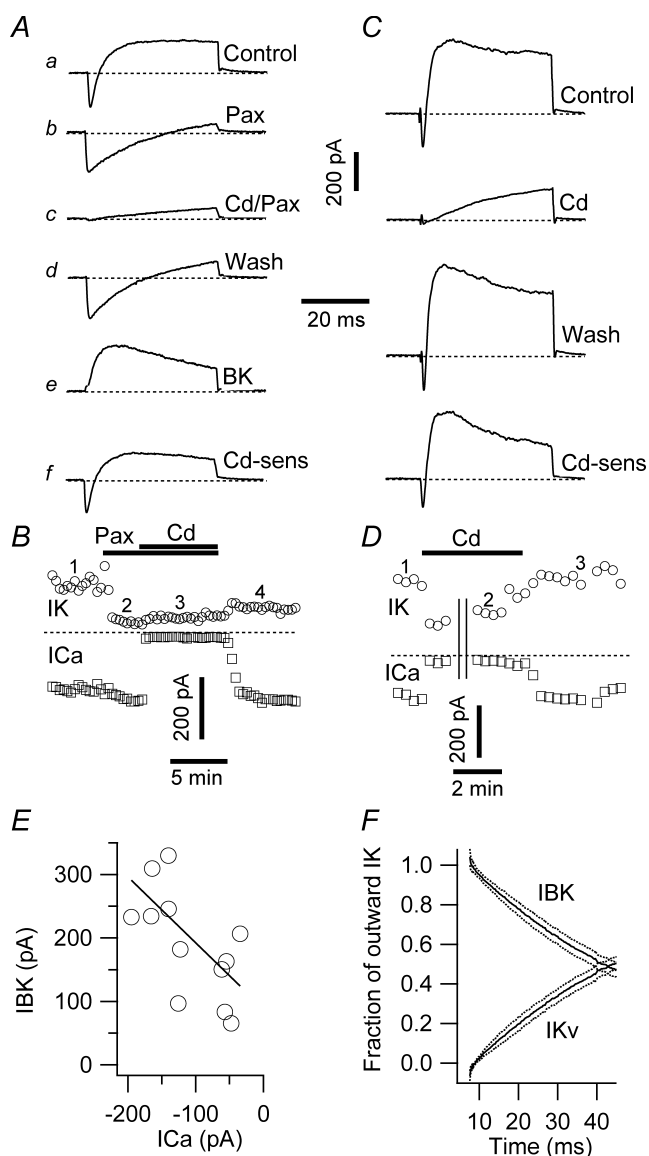
Figure 2. Identification of I_{BK} in voltage-clamped β-cells
A, membrane currents recorded in response to P1 command. *a* was recorded in 5 mM glucose and 200 μM tolbutamide. *b* was recorded in the added presence of 1 μM paxilline; *c* was recorded in the added presence of 200 μM Cd^{2+}. *d* shows full recovery of inward current and partial recovery of the outward current upon return to 'Control' solution. *e* shows the paxilline-sensitive I_{BK}, obtained by subtraction of *b* from *a*. *f* shows Cd^{2+}-sensitive current, obtained by subtraction of *c* from *a*. *B*, time course of the experiment illustrated in *A*. Circles and squares denote the peak outward I_K and inward I_{Cav} currents, respectively. The numbers above the graph depict the approximate positions for *a, b, c* and *d* shown in *A*. The horizontal bars indicate periods of paxilline and Cd^{2+} application. *C*, membrane currents, recorded in a different β-cell. 'Control' trace was recorded in solution containing 5 mM glucose and 200 μM tolbutamide. 'Cd' trace was recorded in the presence of 200 μM Cd^{2+} to block I_{Cav} and Ca^{2+}-dependent currents. 'Wash' trace shows full recovery of inward and outward current components upon return to Control solution. 'Cd-sens' trace shows Cd^{2+}-sensitive current (I_{BK}, I_{Cav} and potentially other Ca^{2+}-sensitive currents) obtained by subtraction of Cd from Control traces. The calibration bar is the same as in *A*. *D*, time course of experiment in *C*. Circles and squares denote peak outward and

interval duration in 11.1 mM glucose was 106.31 ± 18.85 s ($n = 16$), and 94.80 ± 14.55 s ($n = 16$) in paxilline; this difference was also not statistically significant ($P = 0.63$). In terms of duty cycle, islets spent on average 62.7% of the time bursting in 11.1 mM glucose alone, and 63.1% when paxilline was present.

Paxilline changed the baseline potential immediately preceding each AP by a statistically insignificant -0.5 ± 0.9 mV, but significantly potentiated the AP peak by 20.3 ± 3.0 mV ($n = 6$; $P < 0.0001$; Fig. 1*B*). Consequently, BK channel blockade in islets exposed to 11.1 mM glucose resulted in increased AP height, but did not alter burst dynamics.

The effect of BK channel block on glucose-dependent APs in single β-cells

In contrast to the bursting behaviour seen in intact islets, elevated glucose triggers continuous AP firing in most single β-cells, with a minority of cells showing a variety of bursting behaviours (Smith *et al.* 1990*a*; Ammala *et al.* 1991; Kinard *et al.* 1999). To test whether the effects of paxilline on APs in whole islets were recapitulated in isolated single β-cells, membrane potential was recorded in 11.1 mM glucose in the absence and presence of 1 μM paxilline (Fig. 1*C*). Analysis of 751 APs in 11.1 mM glucose and 352 APs in the added presence of paxilline showed that paxilline enhanced AP peak height by an average of 15.6 ± 0.5 mV, a difference which was highly significant ($P < 0.0001$) in each of the four β-cells tested. In contrast, paxilline had no significant effect on baseline potential (0.1 ± 1.0 mV).

Figure 1*D* shows two exemplar APs, selected from the trace in Fig. 1*C*, plotted on an expanded time scale and manually aligned so that their peaks coincided temporally. The dotted-line AP was recorded in 11.1 mM glucose, and the continuous-line AP was recorded after 1 μM paxilline. Paxilline potentiated AP height, resulting in a positive overshoot, did not affect baseline potential, and did not appear to affect AP width, nor did it inhibit the after-hyperpolarisation (AHP) phase that often follows the AP.

inward currents, respectively. The numbers above the graph depict positions of the traces shown in *C*; the horizontal bar indicates duration of Cd^{2+} application. Both inward and outward currents were blocked by Cd^{2+} and recovered rapidly upon washout. Parallel vertical lines depict a 255 s break in the recording while other protocols were executed. Dashed lines in *A–D* indicate zero current level. *E*, correlation between I_{Cav} and I_{BK} in individual β-cells. The continuous line shown is a least-square fit to the data with slope −0.9763. *F*, dynamics of the contributions of I_{BK} and I_{Kv} to current elicited by a short depolarizing pulse. The proportion of total outward I_K carried by I_{BK} and I_{Kv}, respectively, are shown as a function of time after the pulse commenced at 5 ms. The continuous lines represent the mean of 12 cells; the dotted lines represent the S.E.M.

I_{BK} mediates a pharmacologically and kinetically distinct component of the outward current activated by a brief depolarisation

Membrane current recorded in single mouse β-cells elicited by a P1 protocol consisted of an early inward component that relaxed outwards (Fig. 2*Aa*). The outward component has been considered to be mainly delayed rectifier I_{Kv} (Smith *et al.* 1990*b*; Roe *et al.* 1996). However, paxilline block revealed that I_{BK} constituted a substantial component of the outward I_K that was larger than the paxilline-insensitive I_{Kv} component (Fig. 2*Ab*).

The early inward current was blocked by 200 μM Cd^{2+} (Fig. 2*Ac*), confirming its identity as I_{Cav} (Satin & Cook, 1985; Rorsman & Trube, 1986; Smith *et al.* 1993; Jing *et al.* 2005). Addition of Cd^{2+} in the presence of paxilline did not decrease I_{Kv} further (compare Fig. 2*Ab* and 2*Ac*). Upon removal of paxilline and Cd^{2+}, I_{Cav} recovered rapidly and fully, whereas I_{BK} recovered slowly and partially (Fig. 2*Ad*). The difference current traces in Fig. 2*Ae* and 2*Af* (Fig. 2*Ab* minus 2*Aa*, Fig. 2*Ac* minus 2*Aa*, respectively) represent I_{BK} and the paxilline- and Cd^{2+}-sensitive current.

The time course of the experiment shown in Fig. 2*A* is plotted in Fig. 2*B*, illustrating that paxilline blocks the I_{BK} component of outward current in a slowly reversible manner, without affecting the inward, Cd^{2+}-sensitive, I_{Cav}. In this experiment, the poor reversibility of paxilline block did not allow us to distinguish whether Cd^{2+} and paxilline were blocking the same I_K component. In an independent set of experiments Cd^{2+}, applied alone, blocked a current grossly indistinguishable from that seen when Cd^{2+} was combined with paxilline (Fig. 2*C*). However, unlike with paxilline, Cd^{2+} block recovered readily upon drug washout (Fig. 2*D*). In pooled data, Cd^{2+} alone blocked $60.0 \pm 11.6\%$ of the peak total outward current ($n = 11$), and in combination with paxilline blocked $60.2 \pm 3.6\%$ ($n = 17$); the two values were not significantly different. I_{Kv} accounted for $38.3 \pm 3.7\%$ of the peak total outward current ($n = 17$). Therefore, 1 μM paxilline blocks the β-cell I_{BK} selectively and completely.

Figure 2*E* depicts peak I_{BK} as a function of the corresponding peak I_{Cav}, determined in 12 separate β-cells, spanning ~5.7- and ~5.0-fold ranges of I_{Cav} and I_{BK}, respectively. The continuous line fit to the data has a slope of -0.9763; I_{Cav} and I_{BK} are significantly correlated ($P = 0.0267$).

Additional pharmacological evidence for a Ca^{2+}-activated I_K was provided by the L-type I_{Cav} blocker nimodipine (1 μM) and the enhancer FPL-64176 (1 μM; McDonough *et al.* 2005), which reduced and enhanced outward current by $15.6 \pm 3.3\%$ ($P = 0.020$; $n = 3$) and $72.2 \pm 38.1\%$ ($P = 0.099$; $n = 3$), respectively.

The scorpion-toxin peptide iberiotoxin (IbTx) is a ChTx analogue that is equally potent at blocking BK channels; unlike ChTx, which was used in an earlier study of BK channels in β-cells (Kukuljan *et al.* 1991), IbTx does not block K_v channels (Galvez *et al.* 1990). In the current study, IbTx blocked $56.2 \pm 12.6\%$ of the paxilline-sensitive I_{BK} current ($n = 4$; individual-cell block ranged from 22.3 to 81.2%).

To compare their activation time courses quantitatively, I_{BK} and I_{Kv} in 12 cells were normalized to the total outward I_K (i.e. $I_{BK} + I_{Kv}$; Fig. 2*F*). I_{BK} carries most of the early repolarizing current (~100%, 2.6 ms into the pulse). Concurrent I_{BK} inactivation and I_{Kv} activation result in either current approaching 50% by the end of the 40 ms pulse.

Taken together, these observations show that I_{BK} constitutes a sizeable component of the outward I_K activated by depolarizing pulses in mouse β-cells, in agreement with our observation that paxilline increased the amplitude of β-cell APs.

Membrane potential- and time-dependence of I_{BK} in β-cells

Time- and voltage-dependence of I_{BK} activation and inactivation were characterized using the IV1 protocol. The multiphasic and noisy currents in Fig. 3*A* were recorded in 5 mM glucose and 200 μM tolbutamide. Paxilline blocked I_{BK}, resulting in outward currents with slower activation, less inactivation and less noise (Fig. 3*B*). I_{Kv} recorded in paxilline and Cd^{2+} activated exponentially (continuous lines superimposed on the current traces; Fig. 3*C*). Subtracting traces in Fig. 3*B* from those in Fig. 3*A* revealed I_{BK} (Fig. 3*D*), characterized by rapid activation, partial inactivation and prominent fluctuations; I_{BK} inactivated mono-exponentially (continuous lines superimposed on current traces). Figure 3*E* shows the paxilline- and Cd^{2+}-sensitive membrane current component obtained by subtracting traces in Fig. 3*C* from those in Fig. 3*A*; addition of Cd^{2+} following paxilline had little effect on outward currents but, as expected, blocked I_{Cav}, so that the subtracted current shown in Fig. 3*E* closely resembles the current in Fig. 3*D*, with an added early inward I_{Cav} component. This early I_{Cav} is shown on an expanded timescale in Fig. 3*G*.

Normalized conductance–voltage (G–V) curves for I_{BK} and I_{Kv} show that both currents activate over a similar membrane potential range (Fig. 4*A*). The dual time constants (τs) for I_{BK} activation and its inactivation τ, have U-shaped membrane potential dependence (Fig. 4*B*); I_{BK} activates at least an order of magnitude faster than I_{Kv} over all but the most depolarised potentials. Figure 4*C* shows the ratio of steady-state I_{BK}, recorded at the end of the 500 ms pulse, to peak I_{BK}. The line fit through the data in the range of -20 to $+30$ mV has a slope of 7.8×10^{-3} mV^{-1}, suggesting that this parameter is slightly voltage dependent.

Therefore, I_{BK} activates with the same voltage dependence, but ~10-fold faster, as I_{Kv}, and inactivates rapidly to a steady-state component that is ~30 to ~60% of the peak.

K$^+$ currents activated by voltage waveforms patterned on APs

To characterize the roles of I_{BK} and I_{Kv} in AP repolarisation, currents were evoked by two voltage commands (AP1 and AP2) patterned on APs recorded in 11.1 mM glucose alone and with paxilline, respectively (Figs 1D, and 5A and B). AP1 evoked a biphasic current (Fig. 5C, black trace) comprising an early transient inward component, followed by a transient outward component. Paxilline (green trace) enhanced the inward component and reduced the outward component. Subsequent Cd^{2+} addition blocked the inward I_{Cav} component, revealing a small transient outward I_{Kv} (blue trace). A transient outward paxilline-sensitive I_{BK} component was obtained by subtraction of the traces. The AP1-activated I_{BK} component was substantially larger than I_{Kv} (red and blue traces in Fig. 5D). In five cells, peak I_{BK} was 7.01 $\pm$ 2.29-fold larger than I_{Kv}. Normalized I_{Kv} and I_{BK} (Fig. 5E) show that I_{Kv} activated ~2 ms slower than I_{BK}, a delay much shorter than observed with the P1 step voltage command (Figs 2–4).

The AP2 command was applied in the presence of paxilline and Cd^{2+} to investigate the I_{Kv}-dependent repolarizing mechanisms in the higher amplitude APs observed in paxilline (Fig. 5B). AP2 activated a dramatically larger (4.11 $\pm$ 0.76-fold; $n = 5$) I_{Kv} than AP1 (Fig. 5F). In a paired comparison, peak amplitude of I_{Kv} activated by AP2 was not significantly different from the peak amplitude of I_{BK} activated by AP1 ($n = 5$; $P = 0.1440$), indicating that the I_{Kv} increase observed with AP2 suffices in repolarizing the AP in the absence of I_{BK}.

AP2 peak is 13 mV more positive than AP1. To determine the contribution of increased conductance (G_{Kv}) or K$^+$ electromotive driving force in the I_{Kv} increase, a point-by-point subtraction of the K$^+$ reversal potential (determined from I_{Kv} tail current protocol; data not shown) from AP commands resulted in driving-voltage (ΔV) waveforms. I_{Kv} was divided by ΔV to produce the G_{Kv} waveform. Comparison of the peak amplitudes of the G_{Kv} and I_{Kv} waveforms activated by AP1 and AP2 revealed
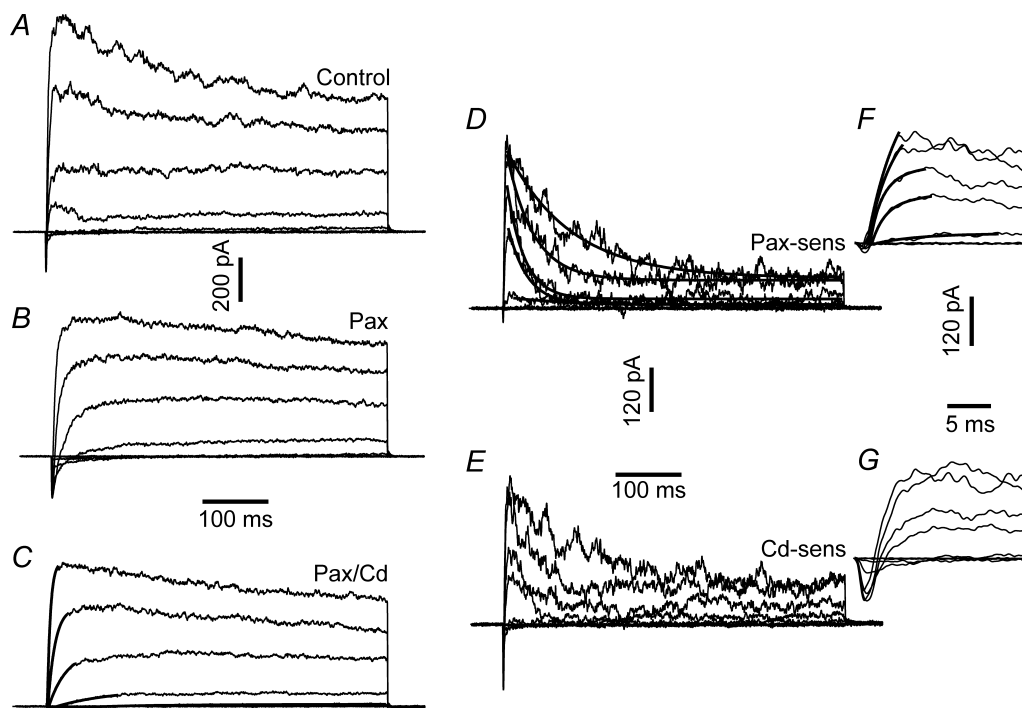

Figure 3. Voltage- and time-dependence of I_{BK} and I_{Kv}
Family of membrane currents activated by IV1 protocol. A, control (5 mM glucose + 200 μM tolbutamide). B, in 1 μM paxilline. C, I_{Kv} recorded in the presence of Cd^{2+} and paxilline. The continuous lines are single exponential fits to the rising phase of the current. D, paxilline-sensitive I_{BK}, obtained by subtracting the currents in B from A. The continuous lines are monoexponential fits of I_{BK} decay. E, Cd^{2+} + paxilline-sensitive current, obtained by subtracting traces in C from A. F, I_{BK} activation. The early phase of I_{BK}, shown in D, is plotted on an expanded time scale. The continuous lines are double exponential fits to I_{BK} rising phase. G, early inward I_{Cav} current. The traces were obtained by plotting the early stages of the traces in E on an expanded time scale. The leftmost calibration bars refer to A, B and C; the middle bars refer to D and E, and the rightmost bars refer to F and G.

that increased G_{Kv} underlay $91.28 \pm 2.17\%$ ($n = 8$) of the I_{Kv} increase, with the remaining $\sim 8\%$ increase due to increased ΔV. This is considerably larger than the $\sim 20\%$ expected from the steady-state G_{Kv} calculated from the step activation experiments illustrated in Fig. 4*A*.
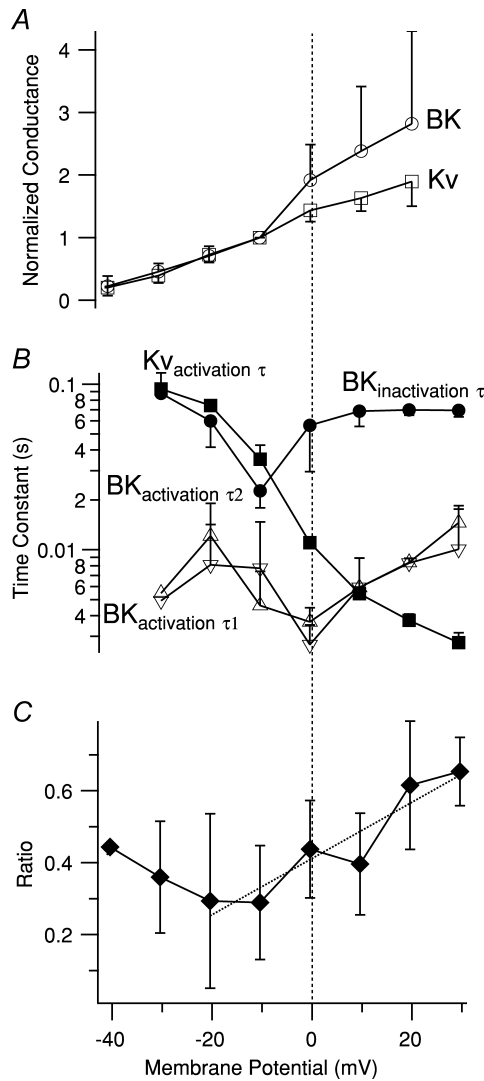

Figure 4. Voltage dependence of amplitude and kinetics of I_{BK} and I_{Kv}

A, normalized conductance–voltage (*G–V*) curves for I_{BK} (open circles) and I_{Kv} (open squares). Each point is the mean ± S.E.M. of 3–4 determinations in different cells normalised to the value at −10 mV. *B*, voltage dependence of the time constant of I_{Kv} activation (Kv$_{activation\tau}$; filled squares), the time constant of I_{BK} inactivation (BK$_{inactivation\tau}$; filled circles), the first time constant of I_{BK} activation (BK$_{activation\tau1}$; upright open triangles), and the second time constant of I_{BK} activation (BK$_{activation\tau2}$; inverted open triangles). Each point is mean ± S.E.M. of 3–4 determinations. Note logarithmic axis for τs. *C*, voltage dependence of ratio of steady-state I_{BK} current (average of I_{BK} over the last 100 ms of the 500 ms pulse) to peak I_{BK}. Each point is the average of 3–4 measurements in separate cells, except the leftmost point, which is a single determination. The dotted line is a linear fit to the data between −20 and +30 mV; its slope is 0.0078 mV^{-1}. The membrane potential axis is the same for all panels; the vertical dashed line denotes 0 mV.
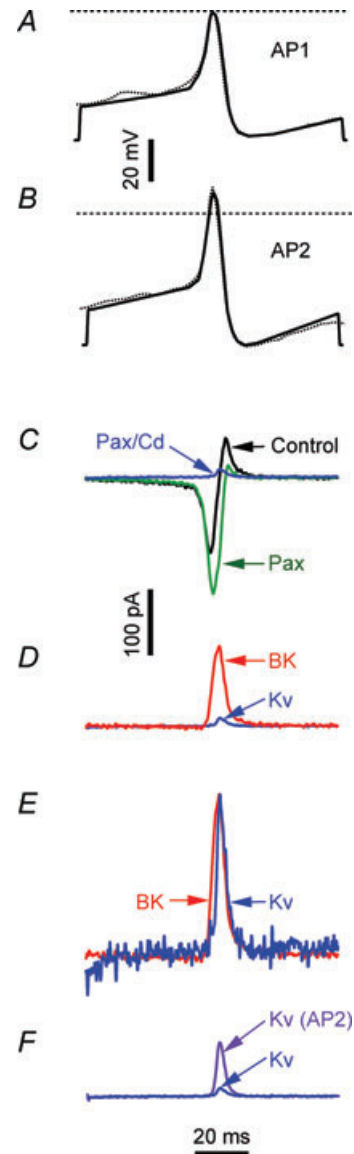
Figure 5. Activation of I_{BK} and I_{Kv} by waveform commands patterned on β-cell APs

The waveform in *A*: low amplitude AP1 command (continuous line) patterned on the AP (dotted line), recorded in 11.1 mM glucose, shown in Fig. 1*D*. *B*, high amplitude AP2 command (continuous line) patterned on the high amplitude AP, recorded in 11.1 mM glucose and 1 μM paxilline, shown in Fig. 1*B*. Voltage calibration bar refers to *A* and *B*. *C*, membrane currents activated by AP1. 'Control' (black) was recorded in 5 mM glucose and 200 μM tolbutamide. 'Pax' (green) was recorded after 1 μM paxilline. 'Pax/Cd' (blue) was recorded in 1 μM paxilline and 200 μM Cd^{2+}. *D*, comparison of I_{BK} and I_{Kv} activated by AP1. 'BK' (red) is the paxilline-sensitive I_{BK} component, obtained by subtracting 'Pax' from 'Control' in *A*. 'Kv' (blue) is I_{Kv}, the current remaining after paxilline and Cd^{2+} have blocked I_{BK} and I_{Cav}; it is identical to the 'Pax/Cd' trace in *C*. *E*, comparison of I_{BK} and I_{Kv} activation and deactivation time courses. I_{BK} ('BK'; red) and I_{Kv} ('Kv'; blue) have been normalized to their respective peaks (arbitrary amplitude scale). *F*, AP2 command enhances I_{Kv} activation. 'Kv' (blue) is the same I_{Kv} trace marked 'Pax/Cd' and 'Kv', in *C* and *D*, respectively. 'Kv AP2' (purple) is I_{Kv} elicited by AP2 command. Current calibration bar refer to *C*, *D* and *F*; vertical calibration of *E* is arbitrary; the time calibration bar refers to all the panels.

Thus, because the change in peak AP height observed in paxilline occurs over a potential range where the G_{Kv} is steeply voltage dependent, the enhanced activation of I_{Kv} compensates for the loss of I_{BK} as a repolarizing mechanism.

Ca²⁺ currents activated by voltage waveforms patterned on APs

AP1 and AP2 were applied in the presence of K⁺ channel blockers to characterize the waveform of I_{Cav} under-
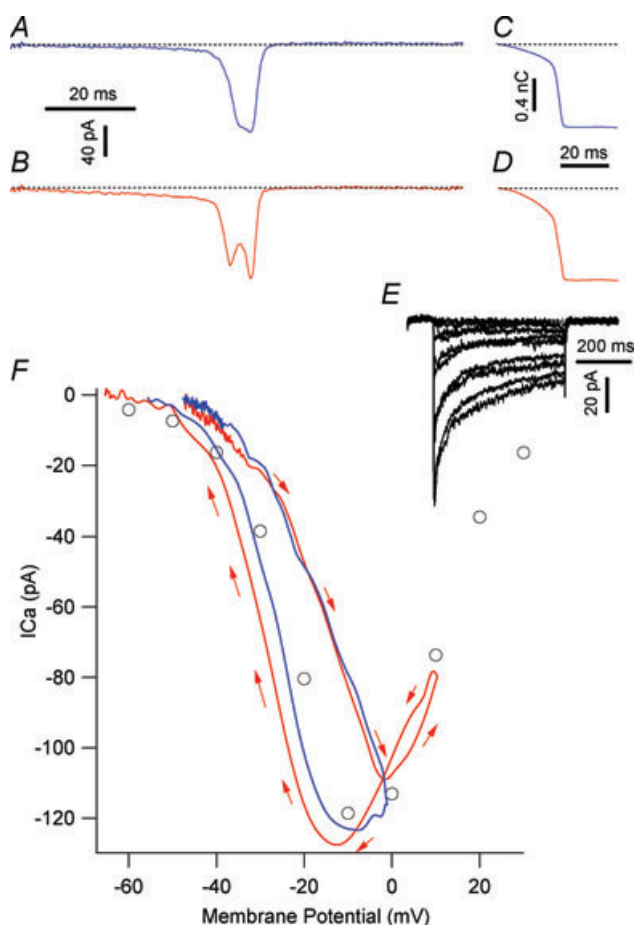

Figure 6. I_{Cav} activation by AP-waveform commands
I_{Cav} activated by AP1 (*A*) and AP2 (*B*) commands. *C* and *D* show the corresponding cumulative Ca²⁺ influx (Q_{Cav}). The dashed lines indicate the zero I_{Cav} or Q_{Cav}. *E*, a family of I_{Cav} traces activated by IV1 protocol, recorded in the same cell as panels *A* and *C*. *F*, comparison of I_{Cav} waveforms activated by AP commands and step depolarisations. Circles represent the voltage dependence of peak I_{Cav} traces activated by the depolarizing steps in *E*. Blue and red curves represent the I_{Cav}s activated by AP1 and AP2, plotted as a function of their voltage waveforms. The red arrows illustrate the direction of the current progression with time in response to AP2 command. Both currents loop clockwise, beginning and ending at the top left corner of the panel; the current activated by AP2 (red trace) has an additional anticlockwise loop, covering ∼−5 to +15 mV potential range, nested within the main current loop.

lying the AP upstroke and to investigate whether the increase in AP height seen in paxilline was associated with changes in Ca²⁺ influx. AP1 and AP2 evoked I_{Cav}s with multiple peaks (Figs 6*A* and *B*, and 7) that had similar maximum amplitudes. I_{Cav} activated by AP1 had a broad staircase-like peak; AP2-evoked I_{Cav} had twin peaks separated by a prominent trough. AP2 elicited more Ca²⁺ influx, calculated as Q_{Cav}, the time integral of I_{Cav} (Fig. 6*C* and *D*). In paired recordings, AP2 significantly increased Q_{Cav} (11.91 ± 4.29%; $n = 4$; $P = 0.037$). Additionally, the traces in Fig. 6*C* and *D* show that a substantial fraction of I_{Cav} activated during the slow depolarisation preceding the AP threshold. This slow I_{Cav} component carried 27.03 ± 5.64% and 33.78 ± 6.02% of the total Q_{Cav} activated by AP1 and AP2, respectively ($n = 4$). Thus, inhibition of I_{BK} enhances Ca²⁺ influx per AP, which may subsequently raise [Ca²⁺]$_i$ and potentiate insulin exocytosis.

Figure 6*E* shows a set of I_{Cav}s activated by the IV1 step protocol recorded in the same cell as panels *A* and *C*. I_{Cav}s activated by IV1 were biophysically similar to those previously reported for β-cells (Satin & Cook, 1985; Rorsman & Trube, 1986). Figure 6*F* compares trajectory of I_{Cav}s evoked by AP1 and AP2 plotted as a function of voltage to the I–V relation of peak I_{Cav}s obtained from the IV1 protocol. I_{Cav}s activated by AP commands show more complex time- and voltage-dependence than expected from the I–V relation. In all four cells examined, both AP1 and AP2 evoked I_{Cav}s that displayed prominent hysteresis; thus, at any membrane potential, more I_{Cav} was activated on the AP downstroke than the upstroke.

BK channel block enhances glucose-stimulated insulin secretion in islets

As I_{BK} enhanced Ca²⁺ entry during APs, we determined whether paxilline enhanced GSIS. Basal insulin secretion rate, measured in 2.8 mM glucose, was not significantly affected by paxilline (0.028 ± 0.005 and 0.032 ± 0.006 ng (100 islets)⁻¹ min⁻¹ in the absence and presence of 1 μM paxilline, respectively; $P > 0.05$). In contrast, in the presence of a stimulatory glucose concentration (11.1 mM), 1 μM paxilline significantly enhanced insulin secretion by approximately 67%, from 0.576 ± 0.110 to 0.960 ± 0.211 ng (100 islets)⁻¹ min⁻¹ ($P = 0.0148$).

Discussion

We report that BK channels activate under physiological conditions and regulate AP amplitude, Ca²⁺ entry and GSIS in mouse pancreatic β-cells. I_{BK} activates over a similar membrane potential range as I_{Kv}; however, it activates more rapidly and inactivates partially; thus, it

carries most of the outward current during the initial phases of the AP. Compared to previous studies (Smith *et al.* 1990*b*; Kukuljan *et al.* 1991), our results suggest a more important role for I_{BK}, and a reappraisal of the role of I_{Kv}, in β-cell function, and posit that I_{BK} serves a similar role in modulating AP shape and GSIS in mouse as it does in human β-cells (Braun *et al.* 2008).

While the I_{BK}s in the present study are kinetically similar to previous reports (Smith *et al.* 1990*b*; Kukuljan *et al.* 1991), our observation that I_{BK} constituted >50% and >85% of outward I_K activated by P1 and AP1, does not support the previous conclusion that BK channels play at most a minor role in AP regulation (Smith *et al.* 1990*b*). Similarly, our observation that paxilline enhanced AP height by ∼21 mV contrasts with the report that ChTx did not affect glucose-stimulated electrical activity in individual β-cells and whole islets (Kukuljan *et al.* 1991).

I_{BK}s and APs recorded in the present study are somewhat larger than reported previously (Smith *et al.* 1990*b*; Kukuljan *et al.* 1991). Mouse strain-dependent differences in BK- and Ca$_v$-channel expression, or the elevated recording temperature and intracellular milieu-preserving perforated patch technique, may have facilitated I_{Cav} and contributed to enhanced I_{BK} amplitudes in the present study (Fig. 2*E*). In addition, use of ChTx by Kukuljan *et al.* (1991) may have led these authors to underestimate

the amplitude and role of I_{BK}. ChTx and IbTx are large charged peptides whereas paxilline is a small lipid-soluble molecule. Therefore, paxilline may have accessed the islet interior better and exerted a bigger effect on APs and GSIS, as has been reported for other tissues (Hu *et al.* 2001; Imlach *et al.* 2010). Moreover, use of ChTx and IbTx in previous studies may have led to underestimation of I_{BK}, as we found that IbTx only partially blocked the paxilline-sensitive I_{BK} in mouse β-cells. Parenthetically, the variable (22% to 81%) IbTx-mediated blockade of β-cell I_{BK}, as well as BK inactivation, may reflect the heterogeneous stoichiometry of β-subunits of the underlying BK channels. Inclusion of β1-, β2- and β4-subunits have been shown to reduce ChTx/IbTx potency by ∼11-, ∼50- and >1000-fold, respectively (Wallner *et al.* 1999; Lippiat *et al.* 2003), whereas paxilline appears able to equally block all known BK channel stoichiometries (Hu *et al.* 2001; Imlach *et al.* 2010). BK channels containing β2- or β3-subunits also inactivate rapidly (Xia *et al.* 1999, 2003). Therefore, if a β-cell expresses multiple β-subunits, the resulting macroscopic I_{BK} may exhibit both inactivating and IbTx-insensitive components (Ding *et al.* 1998). The BK channel β-subunit expression profile of mouse primary β-cells is unknown; however, an insulinoma expresses mRNA of the β3 subunit (Xia *et al.* 1999), and human β-cells express mRNAs for both β2
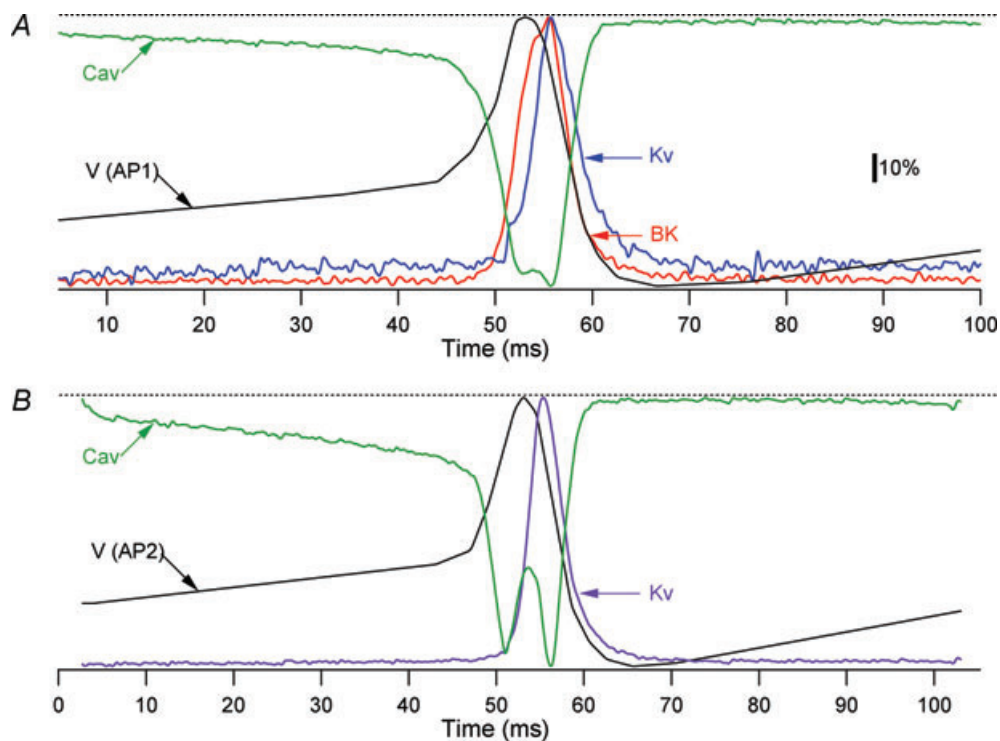

Figure 7. Temporal alignment of membrane voltage and normalized currents activated by AP1 (*A*) and AP2 (*B*)

Colour coding for the I_K traces is as in Fig. 5. In both panels, black traces marked V (AP1) and V (AP2) represent membrane voltage and green traces marked Cav represent I_{Cav}. Dashed lines show zero level for I_{Cav} and maximum level for I_{Kv}, I_{BK} and membrane voltage. The calibration bar refers to both panels.

and $\beta 3$ (Braun *et al.* 2008). In summary, quantitative technical issues may help account for the discrepancies between earlier studies and the conclusions of the present study.

The multiple peaks in I_{Cav}s activated by AP commands (Figs 6 and 7) are qualitatively similar to those reported in an insulinoma cell line (Li *et al.* 1999). Differences in activation and deactivation rates of the underlying Ca_v channel subtypes may have caused time-dependent changes in the composition of the macroscopic I_{Cav}s, resulting in the hysteresis shown in Fig. 6*F* (Chan *et al.* 2005).

BK channel block increased Ca^{2+} influx into the β-cells by $\sim 12\%$ and enhanced GSIS by $\sim 67\%$. A single AP may raise $[Ca^{2+}]$ at the secretory apparatus sufficiently to trigger exocytosis (Ammala *et al.* 1993). Insulin secretion is steeply dependent on $[Ca^{2+}]_i$ in the physiological range (Hill coefficient $= 3.4$; Renstrom *et al.* 1997). This is also reflected in the observation that secretion rate increased 3-fold from -20 to $0\,mV$ (Gopel *et al.* 2004), a similar voltage range over which the AP peaks are enhanced by paxilline. Thus, the increase in Q_{Cav} could in principle account for the $\sim 67\%$ increase in GSIS associated with I_{BK} block. Moreover, the substantial Ca^{2+} influx that precedes AP threshold may stimulate insulin vesicle priming or exocytosis from the highly Ca^{2+}-sensitive pool (Gromada *et al.* 1999; Neher & Sakaba, 2008).

The results of the present study suggest a modification of the current model of AP generation in the β-cell. Figure 7*A* shows normalized I_{BK}, I_{Kv} and I_{Cav}, activated by AP1, averaged from four to five β-cells and aligned with voltage trace. Figure 7*B* shows the corresponding I_{Kv} and I_{Cav} activated by AP2 and aligned with voltage trace.

In $11.1\,mM$ glucose, a depolarisation beyond the AP threshold triggers a sharp increase in I_{Cav} that depolarizes the membrane rapidly. The depolarisation and Ca^{2+} influx activate I_{BK}, beginning $\sim 4\,ms$ after the AP threshold and coinciding with the last $\sim 3\,ms$ of the AP upstroke (Fig. 7*A*). I_{BK} activation slows the depolarization rate and truncates the AP. The slower I_{Kv} activates with a further $\sim 2\,ms$ delay, coinciding with the last $\sim 1\,ms$ of the AP upstroke. As I_{Kv} is slower and 7-fold smaller than I_{BK} (Fig. 5*D*), it minimally affects the AP upstroke and peak amplitude. I_{BK} and I_{Kv} peak $\sim 3\,ms$ after the AP peak and underlie the downstroke. The larger I_{BK} dominates early repolarisation; however, I_{BK} turns off faster than I_{Kv}, which is consistent with the latter contributing preferentially to the later stages of downstroke and the AHP.

In paxilline (Fig. 7*B*), I_{BK} block eliminates a major part of the early repolarising drive, allowing I_{Cav} to depolarise the membrane further, and resulting in a taller AP. However, increased depolarisation increases G_{Kv} and K^+ driving force, and accelerates I_{Kv} activation, resulting in a 4-fold increase in peak I_{Kv} than that activated by AP1 command. Along with I_{Cav} inactivation and decreased

Ca^{2+} driving force (Fig. 6*E*), this larger I_{Kv} serves to repolarise the AP and underlies the AHP.

Our results and model for the distinct roles of I_{BK} and I_{Kv} in AP repolarisation and AHP generation are consistent with previous studies of I_K in β-cells. Thus, while the I_{Kv} in β-cells is mostly carried by $K_v 2.1$ channels (Roe *et al.* 1996; MacDonald *et al.* 2002; Herrington *et al.* 2006; Herrington, 2007; Jacobson *et al.* 2007) absence of this current does not prevent AP repolarisation (Jacobson *et al.* 2007). Instead, a specific $K_v 2.1$ blocker broadens (>2-fold) the AP and inhibits the AHP, while only marginally affecting the AP amplitude (Herrington *et al.* 2006; Herrington, 2007). Similarly, genetic ablation of $K_v 2.1$ reveals a transient outward current that is remarkably similar in its amplitude and kinetics to the I_{BK} described in the present study (see Figs 2 and 3 of Jacobson *et al.* (2007)). Thus, it is conceivable that the remaining outward current in $K_v 2.1$-knockout β-cells is carried by BK type channels. This remains to be determined in future studies.

In conclusion, this study demonstrates that BK channels in the mouse β-cell activate under physiological conditions, and modulate glucose-dependent electrical activity and insulin secretion, raising the possibility that inherited BK channel defects (Du *et al.* 2005) may have metabolic consequences. As BK channels are modulated by multiple signalling mechanisms (Hou *et al.* 2009), this mechanism has the potential to dynamically integrate, on an AP-by-AP basis, multiple cellular signalling pathways, such as those triggered by neurotransmitters or incretin hormones, to modulate GSIS by up to 67%. In addition, the wide variety of drugs that modulate BK channel function (Nardi *et al.* 2003; Nardi & Olesen, 2008) could provide a novel approach for modulating GSIS in diabetic and hyperinsulinaemic patients.

References

Adelman JP, Shen KZ, Kavanaugh MP, Warren RA, Wu YN, Lagrutta A, Bond CT & North RA (1992). Calcium-activated potassium channels expressed from cloned complementary DNAs. *Neuron* **9**, 209–216.

Ammala C, Eliasson L, Bokvist K, Larsson O, Ashcroft FM & Rorsman P (1993). Exocytosis elicited by action potentials and voltage-clamp calcium currents in individual mouse pancreatic B-cells. *J Physiol* **472**, 665–688.

Ammala C, Larsson O, Berggren PO, Bokvist K, Juntti-Berggren L, Kindmark H & Rorsman P (1991). Inositol trisphosphate-dependent periodic activation of a Ca^{2+}-activated K^+ conductance in glucose-stimulated pancreatic beta-cells. *Nature* **353**, 849–852.

Ashcroft FM & Rorsman P (1989). Electrophysiology of the pancreatic beta-cell. *Prog Biophys Mol Biol* **54**, 87–143.

Atwater I, Dawson CM, Ribalet B & Rojas E (1979). Potassium permeability activated by intracellular calcium ion concentration in the pancreatic beta-cell. *J Physiol* **288**, 575–588.

Atwater I, Rosario L & Rojas E (1983). Properties of the Ca-activated K$^+$ channel in pancreatic beta-cells. *Cell Calcium* **4**, 451–461.

Bokvist K, Rorsman P & Smith PA (1990). Block of ATP-regulated and Ca^{2+}-activated K$^+$ channels in mouse pancreatic beta-cells by external tetraethylammonium and quinine. *J Physiol* **423**, 327–342.

Braun M, Ramracheya R, Bengtsson M, Zhang Q, Karanauskaite J, Partridge C, Johnson PR & Rorsman P (2008). Voltage-gated ion channels in human pancreatic beta-cells: electrophysiological characterization and role in insulin secretion. *Diabetes* **57**, 1618–1628.

Butler A, Tsunoda S, McCobb DP, Wei A & Salkoff L (1993). mSlo, a complex mouse gene encoding "maxi" calcium-activated potassium channels. *Science* **261**, 221–224.

Chan SA, Polo-Parada L & Smith C (2005). Action potential stimulation reveals an increased role for P/Q-calcium channel-dependent exocytosis in mouse adrenal tissue slices. *Arch Biochem Biophys* **435**, 65–73.

Chay TR (1986). On the effect of the intracellular calcium-sensitive K$^+$ channel in the bursting pancreatic beta-cell. *Biophys J* **50**, 765–777.

Cook DL, Ikeuchi M & Fujimoto WY (1984). Lowering of pH$_i$ inhibits Ca^{2+}-activated K$^+$ channels in pancreatic B-cells. *Nature* **311**, 269–271.

Dean PM & Matthews EK (1968). Electrical activity in pancreatic islet cells. *Nature* **219**, 389–390.

Ding JP, Li ZW & Lingle CJ (1998). Inactivating BK channels in rat chromaffin cells may arise from heteromultimeric assembly of distinct inactivation-competent and noninactivating subunits. *Biophys J* **74**, 268–289.

Drummond GB (2009). Reporting ethical matters in *The Journal of Physiology*: standards and advice. *J Physiol* **587**, 713–719.

Du W, Bautista JF, Yang H, Diez-Sampedro A, You SA, Wang L, Kotagal P, Luders HO, Shi J, Cui J, Richerson GB & Wang QK (2005). Calcium-sensitive potassium channelopathy in human epilepsy and paroxysmal movement disorder. *Nat Genet* **37**, 733–738.

Falke LC, Gillis KD, Pressel DM & Misler S (1989). 'Perforated patch recording' allows long-term monitoring of metabolite-induced electrical activity and voltage-dependent Ca^{2+} currents in pancreatic islet B cells. *FEBS Lett* **251**, 167–172.

Findlay I, Dunne MJ & Petersen OH (1985). High-conductance K$^+$ channel in pancreatic islet cells can be activated and inactivated by internal calcium. *J Membr Biol* **83**, 169–175.

Galvez A, Gimenez-Gallego G, Reuben JP, Roy-Contancin L, Feigenbaum P, Kaczorowski GJ & Garcia ML (1990). Purification and characterization of a unique, potent, peptidyl probe for the high conductance calcium-activated potassium channel from venom of the scorpion *Buthus tamulus*. *J Biol Chem* **265**, 11083–11090.

Goforth PB, Bertram R, Khan FA, Zhang M, Sherman A & Satin LS (2002). Calcium-activated K$^+$ channels of mouse beta-cells are controlled by both store and cytoplasmic Ca^{2+}: experimental and theoretical studies. *J Gen Physiol* **120**, 307–322.

Gopel S, Kanno T, Barg S, Galvanovskis J & Rorsman P (1999*a*). Voltage-gated and resting membrane currents recorded from B-cells in intact mouse pancreatic islets. *J Physiol* **521**, 717–728.

Gopel S, Zhang Q, Eliasson L, Ma XS, Galvanovskis J, Kanno T, Salehi A & Rorsman P (2004). Capacitance measurements of exocytosis in mouse pancreatic α-, β- and δ-cells within intact islets of Langerhans. *J Physiol* **556**, 711–726.

Gopel SO, Kanno T, Barg S, Eliasson L, Galvanovskis J, Renstrom E & Rorsman P (1999*b*). Activation of Ca^{2+}-dependent K$^+$ channels contributes to rhythmic firing of action potentials in mouse pancreatic beta cells. *J Gen Physiol* **114**, 759–770.

Gromada J, Hoy M, Renstrom E, Bokvist K, Eliasson L, Gopel S & Rorsman P (1999). CaM kinase II-dependent mobilization of secretory granules underlies acetylcholine-induced stimulation of exocytosis in mouse pancreatic B-cells. *J Physiol* **518**, 745–759.

Henquin JC & Meissner HP (1984). Significance of ionic fluxes and changes in membrane potential for stimulus-secretion coupling in pancreatic B-cells. *Experientia* **40**, 1043–1052.

Herrington J (2007). Gating modifier peptides as probes of pancreatic beta-cell physiology. *Toxicon* **49**, 231–238.

Herrington J, Zhou YP, Bugianesi RM, Dulski PM, Feng Y, Warren VA *et al.* (2006). Blockers of the delayed-rectifier potassium current in pancreatic beta-cells enhance glucose-dependent insulin secretion. *Diabetes* **55**, 1034–1042.

Hou S, Heinemann SH & Hoshi T (2009). Modulation of BKCa channel gating by endogenous signaling molecules. *Physiology (Bethesda)* **24**, 26–35.

Houamed KM, Fu J, Roe MW & Philipson LH (2004). Electrophysiology of the pancreatic beta cell. In *Diabetes Mellitus*, ed. LeRoith D, Taylor SI & Olefsky JM, pp. 51–68. Lippincott Williams and Wilkins, Philadelphia.

Houamed KM & Satin LS (2009). Multiple components of Ca-activated K currents in mouse pancreatic beta cells. *Biophys J* **96**, 473a.

Hu H, Shao LR, Chavoshy S, Gu N, Trieb M, Behrens R, Laake P, Pongs O, Knaus HG, Ottersen OP & Storm JF (2001). Presynaptic Ca^{2+}-activated K$^+$ channels in glutamatergic hippocampal terminals and their role in spike repolarization and regulation of transmitter release. *J Neurosci* **21**, 9585–9597.

Imlach WL, Finch SC, Miller JH, Meredith AL & Dalziel JE (2010). A role for BK channels in heart rate regulation in rodents. *PLoS One* **5**, e8698.

Jacobson DA, Kuznetsov A, Lopez JP, Kash S, Ammala CE & Philipson LH (2007). Kv2.1 ablation alters glucose-induced islet electrical activity, enhancing insulin secretion. *Cell Metab* **6**, 229–235.

Jing X, Li DQ, Olofsson CS, Salehi A, Surve VV, Caballero J *et al.* (2005). CaV2.3 calcium channels control second-phase insulin release. *J Clin Invest* **115**, 146–154.

Jung SR, Reed BJ & Sweet IR (2009). A highly energetic process couples calcium influx through L-type calcium channels to insulin secretion in pancreatic beta-cells. *Am J Physiol Endocrinol Metab* **297**, E717–E727.

Kaczorowski GJ, Knaus HG, Leonard RJ, McManus OB & Garcia ML (1996). High-conductance calcium-activated potassium channels; structure, pharmacology, and function. *J Bioenerg Biomembr* **28**, 255–267.

Kinard TA, de Vries G, Sherman A & Satin LS (1999). Modulation of the bursting properties of single mouse pancreatic beta-cells by artificial conductances. *Biophys J* **76**, 1423–1435.

Knaus HG, McManus OB, Lee SH, Schmalhofer WA, Garcia-Calvo M, Helms LM *et al.* (1994). Tremorgenic indole alkaloids potently inhibit smooth muscle high-conductance calcium-activated potassium channels. *Biochemistry* **33**, 5819–5828.

Kukuljan M, Goncalves AA & Atwater I (1991). Charybdotoxin-sensitive K_{Ca} channel is not involved in glucose-induced electrical activity in pancreatic beta-cells. *J Membr Biol* **119**, 187–195.

Leung YM, Ahmed I, Sheu L, Tsushima RG, Diamant NE, Hara M & Gaisano HY (2005). Electrophysiological characterization of pancreatic islet cells in the mouse insulin promoter-green fluorescent protein mouse. *Endocrinology* **146**, 4766–4775.

Li ZW, Ding JP, Kalyanaraman V & Lingle CJ (1999). RINm5f cells express inactivating BK channels whereas HIT cells express noninactivating BK channels. *J Neurophysiol* **81**, 611–624.

Lippiat JD, Standen NB, Harrow ID, Phillips SC & Davies NW (2003). Properties of BK(Ca) channels formed by bicistronic expression of hSloα and β1–4 subunits in HEK293 cells. *J Membr Biol* **192**, 141–148.

MacDonald PE, Sewing S, Wang J, Joseph JW, Smukler SR, Sakellaropoulos G *et al.* (2002). Inhibition of Kv2.1 voltage-dependent K^+ channels in pancreatic beta-cells enhances glucose-dependent insulin secretion. *J Biol Chem* **277**, 44938–44945.

MacDonald PE & Wheeler MB (2003). Voltage-dependent K^+ channels in pancreatic beta cells: role, regulation and potential as therapeutic targets. *Diabetologia* **46**, 1046–1062.

McDonough SI, Mori Y & Bean BP (2005). FPL 64176 modification of Ca_V1.2 L-type calcium channels: dissociation of effects on ionic current and gating current. *Biophys J* **88**, 211–223.

Mancilla E & Rojas E (1990). Quinine blocks the high conductance, calcium-activated potassium channel in rat pancreatic beta-cells. *FEBS Lett* **260**, 105–108.

Marty A (1981). Ca-dependent K channels with large unitary conductance in chromaffin cell membranes. *Nature* **291**, 497–500.

Nardi A, Calderone V, Chericoni S & Morelli I (2003). Natural modulators of large-conductance calcium-activated potassium channels. *Planta Med* **69**, 885–892.

Nardi A & Olesen SP (2008). BK channel modulators: a comprehensive overview. *Curr Med Chem* **15**, 1126–1146.

Neher E (1992). Correction for liquid junction potentials in patch clamp experiments. *Methods Enzymol* **207**, 123–131.

Neher E & Sakaba T (2008). Multiple roles of calcium ions in the regulation of neurotransmitter release. *Neuron* **59**, 861–872.

Orio P, Rojas P, Ferreira G & Latorre R (2002). New disguises for an old channel: MaxiK channel beta-subunits. *News Physiol Sci* **17**, 156–161.

Renstrom E, Eliasson L & Rorsman P (1997). Protein kinase A-dependent and -independent stimulation of exocytosis by cAMP in mouse pancreatic B-cells. *J Physiol* **502**, 105–118.

Roe MW, Worley JF 3rd, Mittal AA, Kuznetsov A, DasGupta S, Mertz RJ *et al.* (1996). Expression and function of pancreatic beta-cell delayed rectifier K+ channels. Role in stimulus-secretion coupling. *J Biol Chem* **271**, 32241–32246.

Rorsman P & Trube G (1986). Calcium and delayed potassium currents in mouse pancreatic beta-cells under voltage-clamp conditions. *J Physiol* **374**, 531–550.

Sanchez M & McManus OB (1996). Paxilline inhibition of the α-subunit of the high-conductance calcium-activated potassium channel. *Neuropharmacology* **35**, 963–968.

Satin LS & Cook DL (1985). Voltage-gated Ca^{2+} current in pancreatic B-cells. *Pflugers Arch* **404**, 385–387.

Satin LS, Hopkins WF, Fatherazi S & Cook DL (1989). Expression of a rapid, low-voltage threshold K current in insulin-secreting cells is dependent on intracellular calcium buffering. *J Membr Biol* **112**, 213–222.

Smith PA, Aschroft FM & Fewtrell CM (1993). Permeation and gating properties of the L-type calcium channel in mouse pancreatic beta cells. *J Gen Physiol* **101**, 767–797.

Smith PA, Ashcroft FM & Rorsman P (1990*a*). Simultaneous recordings of glucose dependent electrical activity and ATP-regulated K^+-currents in isolated mouse pancreatic beta-cells. *FEBS Lett* **261**, 187–190.

Smith PA, Bokvist K, Arkhammar P, Berggren PO & Rorsman P (1990*b*). Delayed rectifying and calcium-activated K^+ channels and their significance for action potential repolarization in mouse pancreatic beta-cells. *J Gen Physiol* **95**, 1041–1059.

Tabcharani JA & Misler S (1989). Ca^{2+}-activated K^+ channel in rat pancreatic islet B cells: permeation, gating and blockade by cations. *Biochim Biophys Acta* **982**, 62–72.

Vergara C, Latorre R, Marrion NV & Adelman JP (1998). Calcium-activated potassium channels. *Curr Opin Neurobiol* **8**, 321–329.

Wallner M, Meera P & Toro L (1999). Molecular basis of fast inactivation in voltage and Ca^{2+}-activated K^+ channels: a transmembrane β-subunit homolog. *Proc Natl Acad Sci U S A* **96**, 4137–4142.

Xia XM, Ding JP & Lingle CJ (1999). Molecular basis for the inactivation of Ca^{2+}- and voltage-dependent BK channels in adrenal chromaffin cells and rat insulinoma tumor cells. *J Neurosci* **19**, 5255–5264.

Xia XM, Ding JP & Lingle CJ (2003). Inactivation of BK channels by the NH2 terminus of the β2 auxiliary subunit: an essential role of a terminal peptide segment of three hydrophobic residues. *J Gen Physiol* **121**, 125–148.

Yan J, Olsen JV, Park KS, Li W, Bildl W, Schulte U, Aldrich RW, Fakler B & Trimmer JS (2008). Profiling the phospho-status of the BKCa channel α subunit in rat brain reveals unexpected patterns and complexity. *Mol Cell Proteomics* **7**, 2188–2198.

Zhang M, Goforth P, Bertram R, Sherman A & Satin L (2003). The Ca^{2+} dynamics of isolated mouse beta-cells and islets: implications for mathematical models. *Biophys J* **84**, 2852–2870.

Zhang M, Houamed K, Kupershmidt S, Roden D & Satin LS (2005). Pharmacological properties and functional role of K_{slow} current in mouse pancreatic beta-cells: SK channels contribute to K_{slow} tail current and modulate insulin secretion. *J Gen Physiol* **126**, 353–363.

Author contributions

All authors contributed to the conception, design, analysis and/or interpretation of the data presented in this paper. The electrophysiological experiments were designed by K.M.H. and L.S.S. and carried out by K.M.H. Analysis of the electrophysiological experiments was done by K.M.H. The insulin secretion experiment was designed by K.M.H., L.S.S. and I.R.S., and carried out and analysed by I.R.S. The paper was written by K.M.H., initially in collaboration with L.S.S., and revised with the critical appraisal of I.R.S. All authors approved the final version of the paper for publication.

Acknowledgements